Numerical Simulation of Rocket Engine Internal Flows

Group Representative

Hiroshi Miyajima   Office of Research and Development, National Space Development Agency of Japan, Invited Scientist

Authors

Taro Shimizu   Office of Research and Development, National Space Development Agency of Japan, Engineer

Yamanishi Nobuhiro   Office of Research and Development, National Space Development Agency of Japan, Engineer

In the development of the Japanese H-IIA launch vehicle, we have encountered some fluid dynamical problems on the LE-7A rocket engine. Until today, the development of Japanese rocket engines was largely based on trial & error, i.e.: an iterative cycle of trial design and experimental verification. The main objective of this study is to accelerate the development of rocket engines by utilizing numerical simulations on the internal flow of the engine. This fiscal year, we have focused on the following two problems that we are facing in the development of the LE-7A rocket engine. One is the large side-load generation in the rocket nozzle during the start-up and shut-down transients, which is simulated by solving the compressible Navier-Stokes equations using the RANS method, and the other is unknown unsteady loads on the inducer in the turbopump system, which is simulated by solving the incompressible Navier-Stokes equations using the LES method. As for the side-load of the nozzle, our 3-dimensional simulation has verified the two origins, which are considered to be the most probable by the experiment and mainly 2-dimensional axis-symmetric simulation. The numerical simulation of a rocket turbopump inducer was also carried out. This year, the calculated non-cavitating flow field was compared with the water tunnel experiment and has shown good agreement using the dynamic Smagorinsky model for the turbulent kinetic viscosity. The modeling of cavitating flows is currently underway, as is the optimization of the LES code.

Keywords: rocket engine, rocket nozzle flow, rocket turbopump inducer, LE-7A, RANS, LES

Report of your result

In order to increase the reliability of the LE-7A engine of the H-IIA launch vehicle and apply its knowledge to future space vehicles, we have conducted the numerical simulation of the internal flow of the liquid rocket engine. This year, we focused on two problems: the large side-load generation in the rocket nozzle and the large unsteady stress generated at the inducer. These two studies are presented in the following.

The large side-load generation in the rocket nozzle during the startup and shutdown transients would induce not only the serious trouble at launch, but also the destruction of the engine hardware at sea level tests. In order to avoid the destructive side-load, much work have been done experimentally and numerically to clarify the origin of the side-load generation[1-5]. It is considered that for the parabolic and CTP (compressed truncated perfect) nozzles, the transition of the flow structure, from FSS (free shock separation) to RSS (restricted shock separation) and vise-versa, creates the sudden change of the pressure distribution along the nozzle wall, resulting in the generation of the side-load. So far, this mechanism is explained by the comparison of the experimental data to mainly the 2-dimensional numerical simulation with an assumption of an axis-symmetric flow configuration. However, it is obvious that the actual magnitude of the side load can only be evaluated by performing 3-dimensional numerical simulation.

The side-load generated in the transient flow in the initial configuration of the LE-7A (CTP) nozzle is considered to originate in the following two reasons[2-5]:

1. In the start-up of the engine, the separation line moves downstream. However, during its movement, the separation line stays at a ramp of film cooling ports for a while, and suddenly shifts downstream.
2. The flow structure changes from FSS to RSS at a certain NPR (chamber pressure to ambient pressure ratio).

Corresponding flow patterns are well captured by 2-dimensional axis-symmetric simulation. The side-load is assumed to be generated by the circumferential asymmetry of the transient flow in realistic 3D flow.

The numerical method to solve the Navier-Stokes equations on the unstructured hybrid grid was developed using a finite volume cell vertex scheme and the LU-SGS implicit time integration algorism[6]. The Goldberg-Ramakrishnan model was used to evaluate the turbulent kinetic viscosity. In some unsteady calculations, Newtonian sub-iteration was implemented based on the Crank-Nicholson method to ensure the time accuracy. The nozzle surface is divided by 240~480 in the circumferential direction. The total number

of the grid is about 3 million. The program is coded by MPI, and calculations in the divided regions are done by the different processes. This year, we transplanted the code to the Earth Simulator system and optimized the code for the minimum requirements of the Earth Simulator. Because the unstructured gird is adopted, further tuning of the programs is very difficult.

Fig. 1 shows the Mach number and the wall pressure distribution of the initial LE-7A nozzle at the nozzle plenum condition for NPR=82 and T=3500K. This nozzle has a ramp for film cooling ports, which generate the pressure decrease of the wall. The 2-dimsional simulation has estimated that the pressure decrease of the wall induces the sudden shift of the separation line to downstream and the large side-load can occur during this movement[2,5]. As is shown in fig. 1, 3-dimensional simulation clarified the non-axis-symmetric flow field and the magnitude of the side-load estimated is found to be similar to the experimental data. We also conducted the simulation without the ramp of film cooling ports and observed no significant side load, verifying that the large side-load at NPR=70~90 originated at this ramp.

Another reason of the large side-load is considered to be the transition of the flow structure from FSS to RSS and vise-versa. The decrease of the O/F (mass ratio of oxidizer to fuel) from the nominal value of 6 is one of the possible reason[4] because it changes the specific heat ratio and the Mach number distribution of the flow, which increase the momentum toward the wall. Fig. 2 presents the wall pressure distribution and streamlines of the flow slightly before the transition to RSS. The deformed separation line indicates that the fluid dynamic instability is the key to understand the transition. The order of the side-load generated during the transition is comparable to the experimental data. The mechanism of the flow instability itself is interesting and will be studied further in the near future.

A large eddy simulation (LES) of a rocket turbopump inducer in non-cavitating and cavitating flows was also carried out. The computation takes full account of the interaction between the rotating inducer and the stationary casing by using a multi-frame-of-reference dynamic overset grid approach[7]. A streamline-upwind finite element formulation with second-order accuracy both in time and space is used to discretize the governing equation. It is implemented in parallel by a domain- decomposition-programming model. The evolution of cavitation is represented by the source/sink of vapor phase in the incompressible liquid flow. The pressure-velocity coupling is based on the fractional-step method for incompressible fluid flows, in which the compressibility is taken into account through the low Mach number assumption. The basic design of this inducer is similar to the one used in the LE-7 rocket engine liquid oxygen turbopump. Particular emphasis is placed on the head-flow characteristics at design and off-design conditions and large vortical structures that appear at the latter condition.

The computed pump heads, together with their measured equivalents are plotted in figure 3. Computations at design condition (ø=0.078) and off-design conditions (ø=0.05 and 0.09) were carried out using two types of sub-grid scale (SGS) models. The prediction of the head-flow characteristic at high-flow ratios (ø=0.078 and 0.09) is very poor for simulations using the standard Smagorinsky model (SSM). On the other hand, the head-flow characteristic using the dynamic Smagorinsky model (DSM) agrees fairly well with the measured values. We should also note that an inflexion point exists around ø=0.065 in the measured values. According to measurements using tufts and bubble tracers, at ø=0.065, the rotating backflow region reaches upstream to the pressure transducer that measures the inlet pressure, and extends further upstream as the flow coefficient decreases[8]. Thus, the inlet pressure is measured higher than expected due to the flow rotation, which in result gives a lower pressure coefficient in the measurements. Such results indicate that an accurate prediction of the backflow region is the key to obtain good agreement at low flow coefficients.

For a detailed analysis on the inlet backflow of the inducer at low flow coefficients, computations were carried out using an improved grid (type B) which includes tip clearance (TC) and holds an extended inlet. The SSM was used for the eddy viscosity model.

Figure 4 is the instantaneous meridional velocity (Cm) distribution at z/D_t=-1.85, -0.95, and -0.05 for ø=0.05. Contrary from computational results using our previous grid (type A), the backflow region reaches upstream to the pressure transducer that measures the inlet pressure. It is unclear whether the backflow region continuously appears near the inlet pressure transducer, but our results have shown that approx. 40% of the time this is true. We have also confirmed that the backflow region rotates with the inducer, at a 13% rotational speed of the inducer. This is consistent with experimental results that have shown rotational speeds of 10 to 20% of the inducer.

Figure 5 is the instantaneous backflow vortex pattern (iso-pressure surface) and pressure distribution at z/D_t=-1.2, -0.6, and 0.0 for ø=0.05. The iso-pressure surface was defined at $p/\rho U_t^2$=-0.18. Here, the vortex created by the shear between the inlet flow and the backflow is defined as the "backflow vortex" as in ref. 9. Similar to experimental results where the number of vortices fluctuates between 2 to 8, two large vortices exist at the upstream, and approximately six near the inducer blade. Overall, based on the results of the upstream edge locations and the rotational speed, it can be said that the swirling backflow at the inlet was simulated relatively accurately. The prediction capability of the developed cavitation LES code is currently being tested for flow around an isolat-

ed hydrofoil as well as that in the test inducer. Optimization of the present LES code is also currently underway.

References

[1] Frey, M. and Hagemann, G., "Restricted Shock Separation in Rocket Nozzles," Journal of Propulsion and Power, Vol. 16, No. 3, 2000.

[2] Takahashi, M., Tomita, T., Takahashi, M., Tamura, H., Watanabe, Y. and Tsuboi, M., "Influence of a Gap for Film Cooling on Transient Flow Characteristics of Rocket Engine Nozzles," AIAA 2002-4147.

[3] Watanabe, Y., and Tsuboi, M., "LE-7A Engine Nozzle Problems during Transient Operations," AIAA2002-3841.

[4] Tomita, T., Sakamoto, H., Takahashi, M., Sasaki, M., Hiroshi T., and Tsuboi, M., "Sub-Scale Nozzle Combustion Tests of the LE-7A Engine for Clarification of Large Side-loads(I): Formation of RSS Structure Due to Combustion Condition," AIAA 2002-3842.

[5] Tomita, T., Sakamoto, H., Takahashi, M., Sasaki, M., Hiroshi T., and Watanabe, Y., "Sub-Scale Nozzle Combustion Tests of the LE-7A Engine for Clarification of Large Side-loads(II): Influence of a Step in Nozzle Contour on Side-Load," AIAA 2002-4002.

[6] Kodera, M., Sunami, T., and Nakahashi, K., "Numerical Analysis of SCRAMJET Combusting Flows by Unstructured Hybrid Grid Method," AIAA 00-0886.

[7] Kato, C., Shimizu, H., and Okamura, T., "Large Eddy Simulation of Unsteady Flow in a Mixed-Flow Pump," ASME FEDSM99-7802.

[8] Kurahara, K., Kataoka, D., Yokota, K., and Tsujimoto, Y., "A Study of Swirling Backflow and a Vortex Structure in the Inlet of an Inducer," Transactions of the Japan Society of Mechanical Engineers, Series B, Vol. 64, pp. 1667-1674, 1998, *in Japanese*.
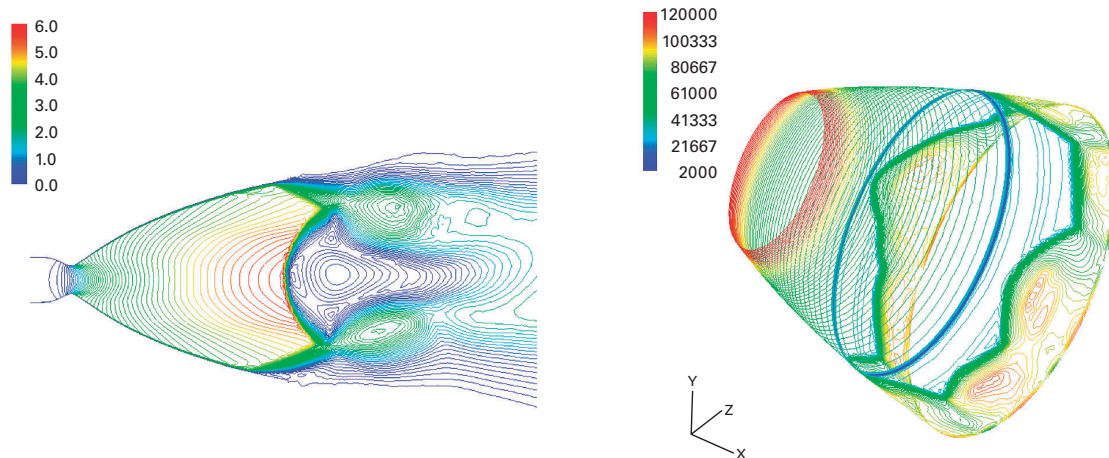
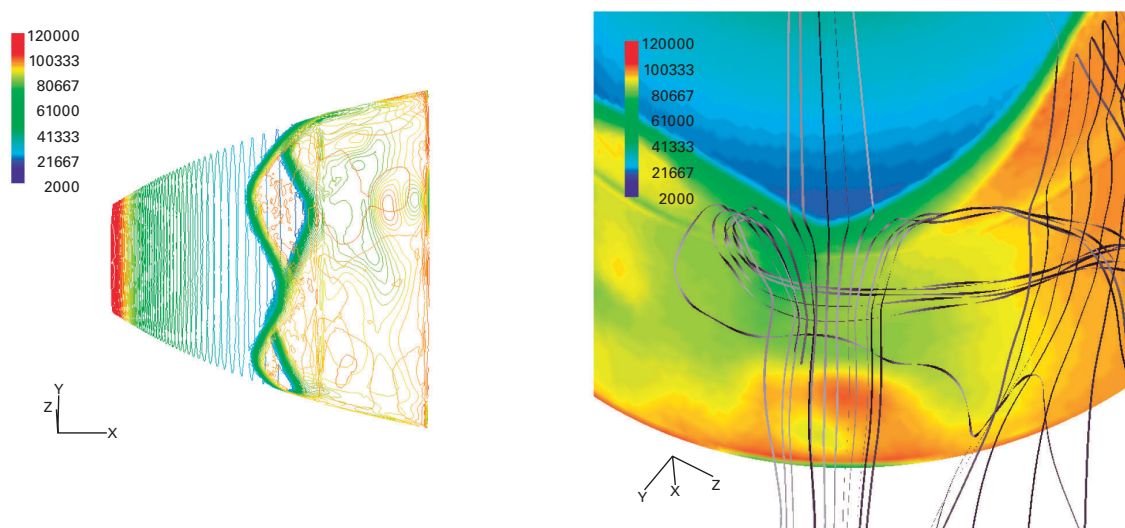Fig. 1 The Mach number (left) and wall pressure Pa (right) distribution at NPR=82 and T=3500K.

Fig. 2 The wall pressure distribution (left) and streamline (right) at NPR=50 and T=3500K under O/F=3.
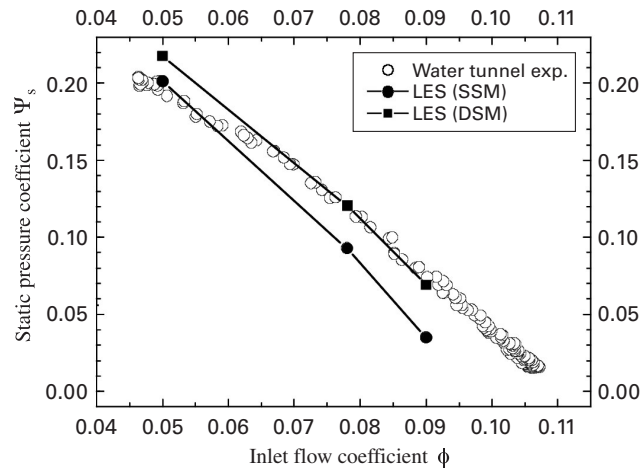
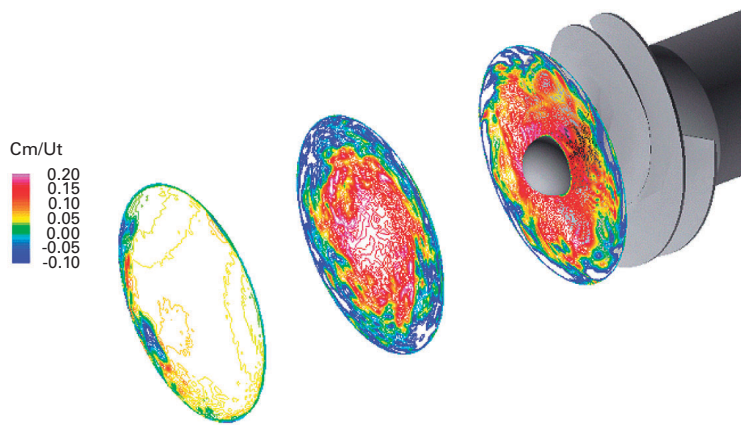Fig. 3 Comparison of measured and predicted head-flow characteristics.

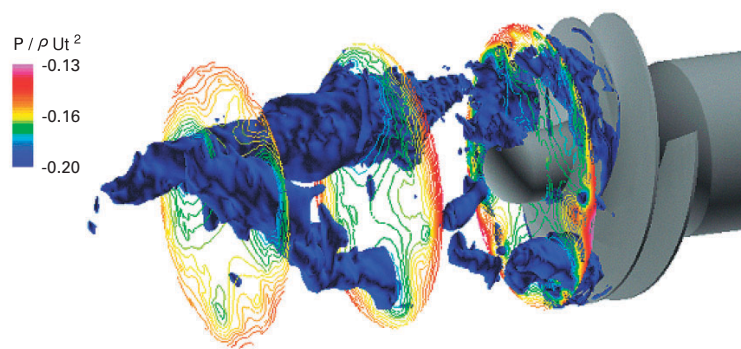Fig. 4 Instantaneous meridional velocity distribution at z/D_t=-1.85, -0.95, and -0.05 (ø=0.05).

Fig. 5 Backflow vortex pattern and pressure distribution at z/D_t=-1.2, -0.6, and 0.0 (ø=0.05).

計算流体力学によるロケットエンジン内部流れの研究

利用責任者

宮島　　博　　　宇宙開発事業団　技術研究本部　招聘研究員

著者

清水　太郎　　　宇宙開発事業団　技術研究本部　開発部員

山西　伸宏　　　宇宙開発事業団　技術研究本部　開発部員

　国産ロケットH-IIAのLE-7Aエンジンおよび将来型宇宙輸送機のエンジンの設計・開発時における諸問題を解決するため、これまで行われてきた実験・試作のサイクルを繰り返す手法に加え、数値計算によってこれらを検証・予測し、開発の効率化を図ることが本研究の目的である。本年度はこのうちLE-7Aエンジンの開発時に問題になった、過大なノズル横力を解明することと、ターボポンプシステムのインデューサで発生する非定常流体力を調べるため、以下の2つのプログラムを用いた解析を行った。ノズル横力の解明では、RANS法を用いてノズル内部流を圧縮性Navier-Stokes方程式により解き、これまで実験や2次元軸対称計算で推測されてきた横力の原因となる2つの要因を明らかにした。ターボポンプ流れの計算では、水流し試験に対応し、流れ場をLES法を用いた非圧縮性Navier-Stokes方程式により解き、ダイナミックスマゴリンスキー乱流モデルを用いた計算で、実験結果との良い一致が得られた。実際の流れで発生しているキャビテーションのモデリング及びLESコードの最適化は現在も実施中である。

キーワード：LE-7Aエンジン、ノズル流れ、ターボポンプ流れ、レイノルズ平均、ラージエディーシミュレーション